

Title	Prediction of electrode properties in Gas Tungsten Arc Welding (GTAW) and Gas Metal Arc Welding (GMAW)
Author(s)	Lowke, J. J.
Citation	Transactions of JWRI. 1996, 25(2), p. 1-8
Version Type	VoR
URL	<a href="https://doi.org/10.18910/8742">https://doi.org/10.18910/8742</a>
rights	
Note	

*Osaka University Knowledge Archive : OUKA*

<https://ir.library.osaka-u.ac.jp/>

Osaka University

# Prediction of electrode properties in Gas Tungsten Arc Welding (GTAW) and Gas Metal Arc Welding (GMAW)

J. J. Lowke.

CSIRO Division of Applied Physics, Sydney, NSW 2070, Australia

## Abstract

*Recent advances in the availability of computers and developments in numerical analysis now make possible numerical predictions of temperatures of the welding electrode in GTAW and GMAW, in a unified arc-electrode treatment. Predictions are made in two dimensions, for any given current, welding gas, and electrode configuration. For GTAW, predictions of surface temperatures of thoriated tungsten electrodes are in fair agreement with temperature measurements made spectroscopically. For GMAW predictions of molten droplet sizes, including the transition current between globular and spray transfer, are in fair agreement with experimental results for argon. Insights have been obtained into the mechanism of the formation of tungsten inclusions in GTAW, effects of molecular gases added to argon welding gas, and the mechanism of the transition current from globular to spray transfer in GMAW.*

## 1. Introduction.

One of the outstanding features of our age is the rapid advances that have been made in the availability of high speed computing power. Coupled with the development of improved methods of numerical analysis, it is now possible to make vastly improved predictions of arc and electrode properties for welding. Among the early significant papers in this subject are several from the Joining and Welding Research Institute, (1) a paper by M. Ushio and F. Matsuda<sup>1)</sup>, which is one of the first predictions of arc temperatures in two dimensions from basic material functions of the arc plasma; and (2) a paper by Matsunawa et al<sup>2)</sup>, which gives one of the first systematic computer predictions of the role of surface tension on the convective flow in the weld pool. This paper analyses the relative influence of the major forces of buoyancy, surface tension, magnetic pinch and viscous drag due to flowing gas, in a way that is only possible using

computers, where, unlike experimental analyses, the influence of the various forces can in turn be set to zero. This paper came to the remarkable conclusion, since verified experimentally<sup>3)</sup>, that the direction of flow in the centre of the weld pool can depend on whether the surface tension increases or decreases with temperature, and has a marked influence on the shape of the weld pool.

Of course an ultimate aim would be the capability of making theoretical predictions in three dimensions so that the properties and strength of a weld produced under any given conditions could be determined. We are a long way from such a capability. However, there is an intermediate scientific benefit in improving our predictive capability which is in many respects more satisfying than even the complete technical capability of providing utilitarian answers to practical problems; namely obtaining insights and understanding of the complex processes that occur in welding. The first page of a noted textbook on numerical analysis by Hamming<sup>4)</sup>

has the motto "The Purpose of Computing is Insight, Not Numbers". A prime example of such valuable insights is the work on surface tension just mentioned<sup>2</sup>.

In the present paper, recent advances are outlined on the prediction of (1) temperatures of thoriated tungsten electrodes in GTAW, (2) properties of the weldpool in GTAW for mixtures of argon and hydrogen as a welding gas compared with pure argon and (3) the size and frequency of metal drops in GMAW. Related to these predictions, insights into three complex welding phenomena are given: (1) the reason the tips of sharp tungsten electrodes can melt off at high current, (2) the role of molecular gases in changing the volume of molten metal in the weld pool for a given arc current, and (3) a simple formula is derived for the transition current from globular to spray transfer in GMAW. It is considered that fairly accurate predictions can be made of arc-electrode interactions when the electrode is thoriated tungsten as in GTAW, or an anode as in GMAW. There are significant uncertainties, however, in treating the cathode region when the cathode is not a thermionic emitter, as is generally the case for the work piece in GMAW.

## 2. Theory

### 2.1 Basic Equations

The basic quantity which is needed for the prediction of welding properties is temperature. If we know the temperature of an electrode we know if it is molten or not. The basic equations defining the temperature are conceptually simple, namely the equations for conservation of mass, energy and momentum<sup>5</sup>. The equation for conservation of mass is

$$\frac{\partial \rho}{\partial t} + \frac{1}{r} \frac{\partial}{\partial r} (r \rho u_r) + \frac{\partial}{\partial z} (\rho u_z) = 0 \quad (1)$$

$\rho$  is the density, and  $u_r$  and  $u_z$  are the radial and axial velocities in the  $r$  and  $z$  directions. The equation for conservation of energy is

$$\begin{aligned} \frac{\partial(\rho h)}{\partial t} + \frac{1}{r} \frac{\partial}{\partial r} (r \rho u_r h) + \frac{\partial}{\partial z} (\rho u_z h) = \\ \frac{1}{r} \frac{\partial}{\partial r} \left( \frac{rk}{c_p} \frac{\partial h}{\partial r} \right) + \frac{\partial}{\partial z} \left( \frac{k}{c_p} \frac{\partial h}{\partial z} \right) + \frac{j_r^2 + j_z^2}{\sigma} - U \end{aligned} \quad (2)$$

$h$  is the enthalpy,  $k$  is the thermal conductivity,  $U$  the radiation emission coefficient,  $c_p$  the specific heat,  $\sigma$  the electrical conductivity, and  $j_r$  and  $j_z$  the radial and axial current densities. The equations for the conservation of radial and axial momentum are

$$\begin{aligned} \frac{\partial(\rho u_r)}{\partial t} + \frac{1}{r} \frac{\partial}{\partial r} (r \rho u_r^2) + \frac{\partial}{\partial z} (\rho u_r u_z) = \\ - \frac{\partial P}{\partial r} - j_z B_\theta + \frac{1}{r} \frac{\partial}{\partial r} \left( 2r \mu \frac{\partial u_r}{\partial r} \right) \\ + \frac{\partial}{\partial z} \left( \mu \frac{\partial u_z}{\partial r} + \frac{\mu \partial u_r}{\partial z} \right) - 2 \mu \frac{u_r}{r^2} \end{aligned} \quad (3)$$

and

$$\begin{aligned} \frac{\partial(\rho u_z)}{\partial t} + \frac{1}{r} \frac{\partial}{\partial r} (r \rho u_z u_r) + \frac{\partial}{\partial z} (\rho u_z^2) = \\ - \frac{\partial P}{\partial z} + j_r B_\theta + \frac{\partial}{\partial z} \left( 2 \mu \frac{\partial u_z}{\partial z} \right) \\ + \frac{1}{r} \frac{\partial}{\partial r} \left( \frac{r \mu \partial u_z}{\partial r} + \frac{r \mu \partial u_r}{\partial z} \right) + \rho g; \end{aligned} \quad (4)$$

$P$  is the pressure,  $\mu$  is the viscosity,  $g$  the gravitational acceleration and  $B_\theta$  the azimuthal magnetic field.  $B_\theta$  is determined from Maxwell's equation

$$\frac{1}{r} \frac{\partial}{\partial r} (r B_\theta) = \mu_0 j_z \quad (5)$$

where  $\mu_0$  is the permeability of free space;  $j = \sigma E$ , where  $E = -\nabla V$  and  $V$  is the potential.

The conservation equations apply separately to the solid electrodes, the molten metal and the arc plasma. The boundaries of these three phases, which in general are all moving, need to be specified on the grid system, and the material functions at each grid point chosen appropriate to each phase and also to the local temperature.

## 2.2 Electrode Plasma Interactions

In the energy balance equation (2), significant energy exchanges occur at the surfaces between the phases, in addition to heat exchange due to thermal conduction. For thermionic cathodes, as is the case for GTAW, there is a strong cooling effect on the tungsten due to electrons leaving the electrode. This energy loss is  $j \phi$  per unit area, where  $\phi$  is the work function of the surface and  $j$  is the current density. Conversely, where electrons enter a surface, as for the welding wire in GMAW, there is a heating effect at the surface of  $j \phi$ . For thermionic cathodes the derived current density at the surface of the cathode may be less than the theoretical current density corresponding to the local temperature. In this case, the difference in current must be supplied by ion current; there will then be a heating effect at such surfaces given by the ion current multiplied by the ionization potential<sup>5</sup>.

## 2.3 Plasma-Electrode Sheath Resistance.

A serious problem arises at all plasma electrode interfaces in that the equilibrium electrical conductivity of the plasma immediately next to the electrode is effectively zero because it is at a temperature that is so low that there is no thermal ionization. Thus if calculations were to consistently assume transport coefficients at the values for local thermal equilibrium, there could be no current, as the thin region in front of the electrodes would have an infinite resistance.

In practice these thin electrode sheath regions do have a finite conductance because (a) for thermionic cathodes there is a finite electron density in the low temperature layer due to thermionic emission and back diffusion of electrons from the plasma, and (b) for the anodes of GMAW and GTAW electrons easily flow across the thin cold layer between the plasma and the anode, with a nonequilibrium electron density. The cold nonequilibrium region is in practice so thin that calculations of gross arc and electrode properties are in fair agreement with experimental results if the sheath regions are completely omitted<sup>6</sup>, provided that the computational mesh size is not taken to be less than 0.005 cm. A more consistent calculation is obtained by calculating the electron density within the

cathode sheath region from ambipolar diffusion<sup>6</sup>, and then evaluating the electrical resistance of the sheath using this electron density. The assumption that space charge sheath effects are small, is supported in that the derived voltages between electrodes are in fair agreement with experimental results<sup>6</sup> and also by recent calculations including an account of space charge effects<sup>7</sup>. There are other authors who believe that the space charge region is very significant, even for thermionic cathodes<sup>8,9</sup>.

## 2.4 Surface Tension Effects.

For GMAW, the welding wire is the anode, which becomes molten to form metal droplets for the weld. The arc and electrode properties vary in time as each drop is produced from the wire and is detached into the arc. The effect of surface tension acting in the surface of the liquid is to compress the drop and effectively increase the pressure inside of the drop by  $P_s$ , where

$$P_s = \gamma \left( \frac{1}{R_1} + \frac{1}{R_2} \right) \quad (6)$$

$\gamma$  is the surface tension coefficient and  $R_1$  and  $R_2$  are the principal radii of curvature of the surface<sup>11</sup>. Thus the effect of surface tension is to introduce in equations (3) and (4) a step function increase in the pressure  $p$  from the plasma to the liquid of an amount given by  $P_s$  from equation (6). For a spherical surface of radius  $R$ , this pressure is  $P_s = 2\gamma / R$ .

## 3. Numerical Predictions

In this section, numerical predictions are given obtained from the basic equations, using material functions of the arc plasma and the electrodes as a function of temperature.

### 3.1 GTAW results for a 200 A arc in argon.

Figure 1 shows predicted temperature contours of a 200A arc in argon with a thoriated tungsten cathode of 60 degree included angle, separated by 5 mm from a copper anode<sup>6</sup>. The back face of the copper is water cooled to main-

## Prediction of Electrode Properties in GTAW and GMAW

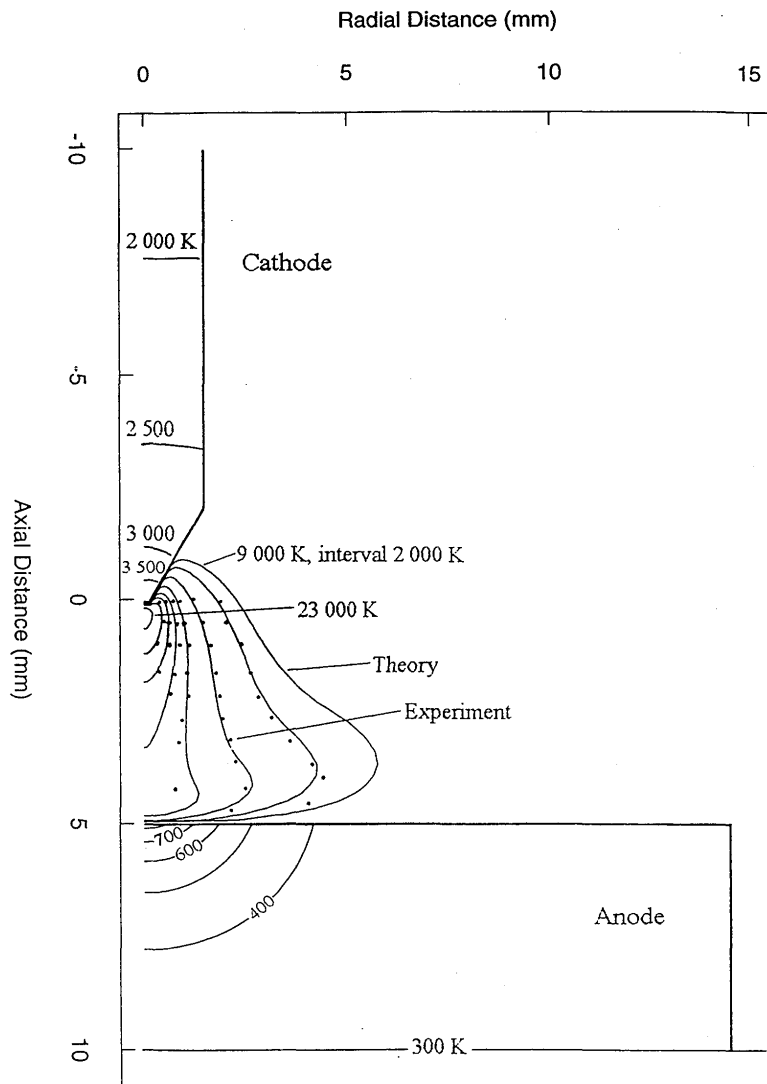


Fig.1 Predicted temperature contours for a 200A arc, compared with experiment [6].

tain it at room temperature, assumed to be 300 K. Experimental values of the arc temperature are shown as points. Figure 2 shows theoretical values of the surface temperature of the tungsten cathode taken from Fig. 1, as a function of distance from the cathode tip. Also shown are experimental values of surface temperature, taken spectroscopically, and shown as points. For both figures the agreement between theory and experiment is very satisfactory.

### 3.2 Influence of 10 % hydrogen in argon on arc and weld pool properties

Figures 3 and 4 show similar calculations to Fig. 1 but with an electrode separation of 3 mm and an anode of mild steel<sup>11)</sup>. Figure 3 is for pure argon and Fig. 4 is for a mixture of argon and 10 %

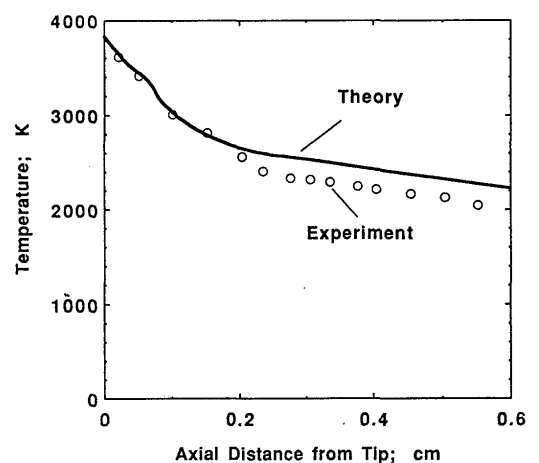


Fig.2 Calculated and experimental cathode surface temperatures [6].

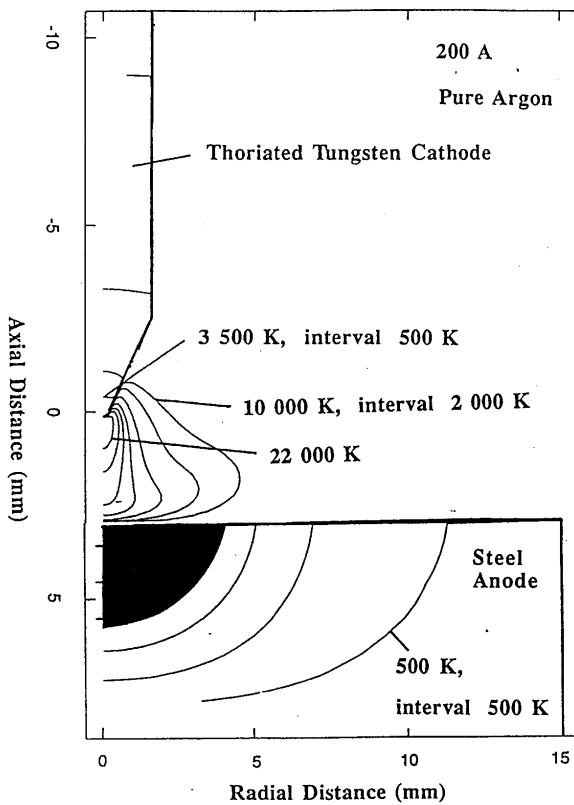


Fig.3 Calculated Contours, 200A, Ar, steel workpiece, molten volume black [11].

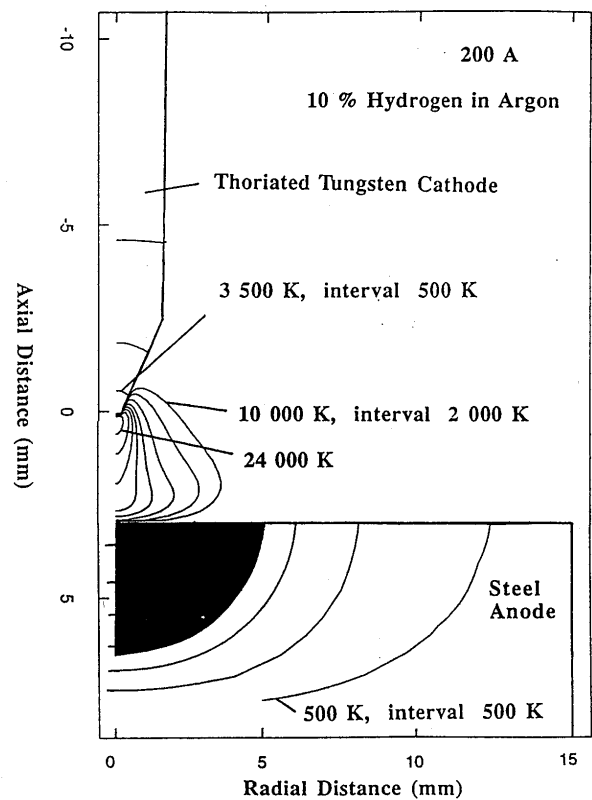


Fig.4 Calculated Contours, 200A, Ar+10% $H_2$  steel workpiece, molten volume black [11].

hydrogen. It is found that the addition of 10 % hydrogen causes a marked increase in the volume of the molten steel, the arc is slightly more constricted and has a slightly increased central temperature and voltage.

### 3.3 GMAW results for droplet and spray transfer.

A feature of GMAW is that for most welding gases there is a discrete mode change in the formation of metal droplets between operation at low and high current<sup>12)</sup>. At low current, in what is called globular transfer, the welding wire melts to produce large liquid drops with a diameter usually larger than the wire diameter. As the current is increased, for most welding gases, there is a transition current above which very much smaller drops are produced of diameter significantly less than that of the wire, in what is called spray transfer. The size of the droplets has a marked influence on the properties of the weld.

Recently predictions have been made of the

time dependence of welding drop formation, again in a unified arc-droplet system, so that predictions of droplet formation for any welding conditions are possible<sup>13)</sup>. These calculations have successfully predicted the large drops corresponding to globular transfer at low current and the small drops, corresponding to spray transfer at high current. Figure 5 shows such a large drop, just before detachment, for a current of 275 A in argon, with a wire diameter of 1.6 mm, and corresponds to globular transfer. Figure 6 shows a small droplet, just before detachment, for a current of 325 A, also in argon for a wire diameter of 1.6mm, and corresponds to spray transfer. For currents near the transition current, the calculations, under some conditions, give a mixture of small and large drops, occurring at different times<sup>13)</sup>.

## 4. Discussion

The numerical calculations given in the previous section make possible various simpli-

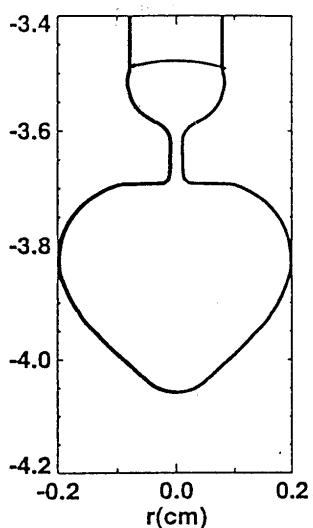


Fig.5 Calculated drop, 275A, 1.6mm wire [13].

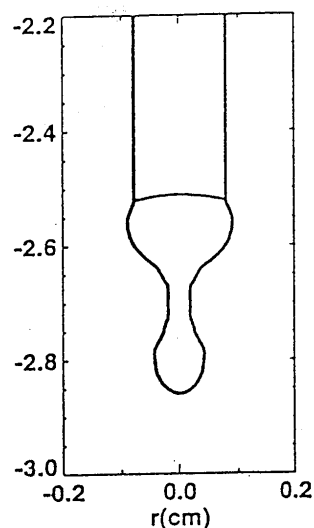


Fig.6 Calculated drop, 325A, 1.6mm wire [13].

fying insights into arc welding processes.

#### 4.1 Cause of tungsten inclusions during GTAW.

If a very high current is passed through the tungsten electrode in GTAW, for example if the electrode accidentally touches the work piece, the tip of the tungsten can "break" off and become embedded in the weld, forming what is known as a tungsten "inclusion". Systematic experimental results<sup>14)</sup> have shown that high currents consistently cause such a tip to detach, as shown in Fig. 7. Surface temperature measurements along the surface of the tungsten, as shown in Figure 8, indicate that there is a maximum in the surface temperature several mm from the tip. Theoretical predictions<sup>6)</sup>, also shown in Fig. 8, also predict a maximum in the surface temperature away from the tip. Thus the tungsten tip actually melts off rather than breaks off and the minimum in the temperature near the tip is due to cooling of the electrode by thermionic emission.

#### 4.2 Influence of the high thermal conductivity of molecular gases in welding arcs.

The only difference in the calculations of Figures 3 and 4 are those of the material functions of argon and argon with 10% hydrogen. These material functions generally differ by only the order of 10%, but with one exception, namely the

values of thermal conductivity. At temperatures of around 3500K, where the dissociation of molecular hydrogen is significant, the thermal conductivity is almost a factor of 10 higher for the mixture than for pure argon. It is this increased thermal conductivity which causes the increased volume of molten metal for the mixture containing hydrogen. The larger thermal conduction also causes a slightly more constricted arc with a higher central temperature and arc voltage.

#### 4.3 Transition current from globular to spray modes of GMAW.

From the detailed calculations of droplet formation of Figs. 5 and 6, it is possible to assess the order of magnitude of the various physical forces influencing drop detachment. The force of surface tension tends to compress the drop and hold it on to the wire. At low currents, magnetic pinch forces due to the self magnetic field of the arc can be neglected and drop sizes grow until gravitational forces overcome the surface tension force tending to hold the drop on to the wire. These drop sizes are larger in diameter than that of the wire, as in globular transfer.

The self magnetic field from the current in the drop exerts a pinch force which tends to increase the pressure inside the drop. For current,  $I$ , flowing in a uniform cylinder of radius  $R$ , Maecker showed<sup>15)</sup> that this magnetic pinch force increases the effective pressure on the axis of the

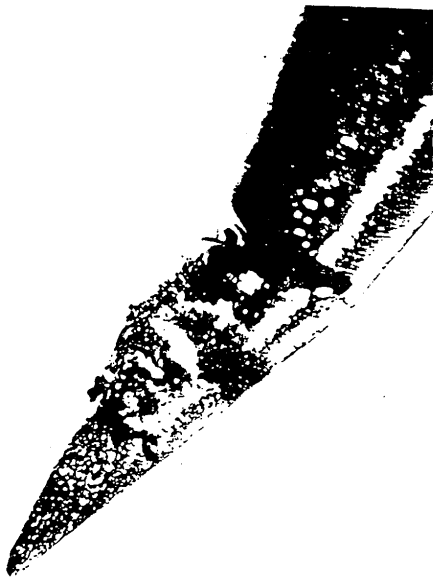


Fig.7 Tungsten cathode melting away from tip at 200A [14].

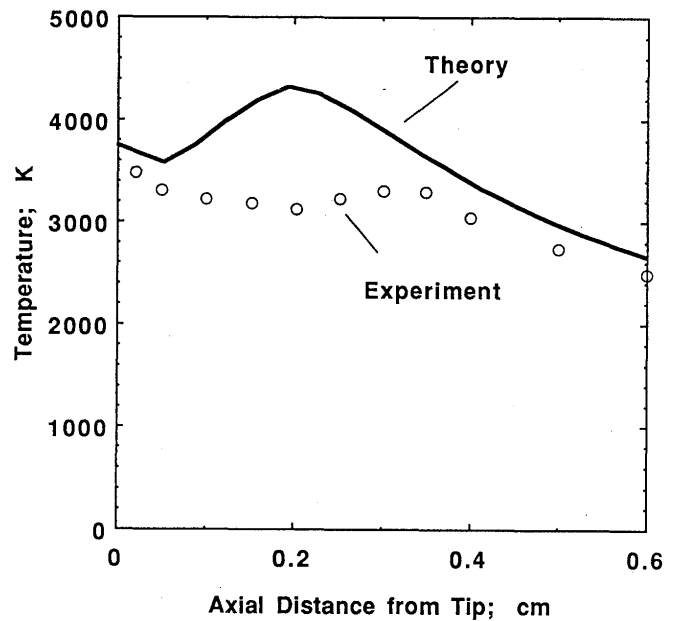


Fig.8 Theoretical and experimental temperatures at 200A for 16 degree tungsten tip [6,14].

cylinder by an amount  $P_m$ , where  $P_m = \mu_0 I^2 / 4\pi^2 R^2$ ;  $\mu_0 = 4\pi 10^{-7} N/A^2$  is the permeability. This pressure increase tends to extrude liquid from the base of the drop, and will tend to reduce the pressure of  $2\gamma/R$  from surface tension holding the hemisphere to the solid wire. As the current increases, the magnetic pinch pressure increases so that there will be a critical current given by  $\mu_0 I^2 / 4\pi^2 R^2 = 2\gamma/R$  beyond which surface tension will no longer be able to support a drop of radius equal to the wire radius. Thus the critical current for transition from the globular mode of transfer to the spray mode of transfer is given by

$$I = 2\pi(2\gamma R / \mu_0)^{1/2} \quad (7)$$

The above derivation is highly approximate in that the effects of gravity, viscous drag forces of the gas surrounding the drop and the pressure of the arc on the drop are all neglected. Figure 9 shows curves of theoretical predictions from Equation (7) for the transition current as a function of wire diameter for mild steel and aluminium. For steel the value of  $\gamma$  was taken as 1.2 N/m and  $\rho$  as 7Mg/m<sup>3</sup> For aluminium the value of  $\gamma$  was taken as 0.28N/m. Experimental values for the transition current are shown as points from references for steel<sup>16-18)</sup> and for alumin-

ium<sup>19)</sup>. The values of  $\gamma$  that have been used have been taken for the boiling point of these metals from Smithell's Metals Reference Book<sup>20)</sup>. It is seen that despite the approximations made in the theory, agreement between theory and experiment is very good. The approximate physical model used to derive equation (7), treated more thoroughly in<sup>21)</sup>, provides a simple physical picture of the reason for the onset of the small droplet mode of spray transfer in GMAW.

### 5. Summary.

Significant progress has recently been made in our capability of making numerical predictions of properties of the electrodes used in GTAW and GMAW. Electrode temperatures derived for GTAW are in fair agreement with experiment and predictions can be made of the main features of droplet transfer in GMAW, including the transition from globular to spray transfer for various conditions. However, we still have a strong need in GMAW to make detailed predictions of the effect of metal drops falling into the weld pool and to treat the work piece, which is a nonthermionic cathode, in a unified way with the arc.



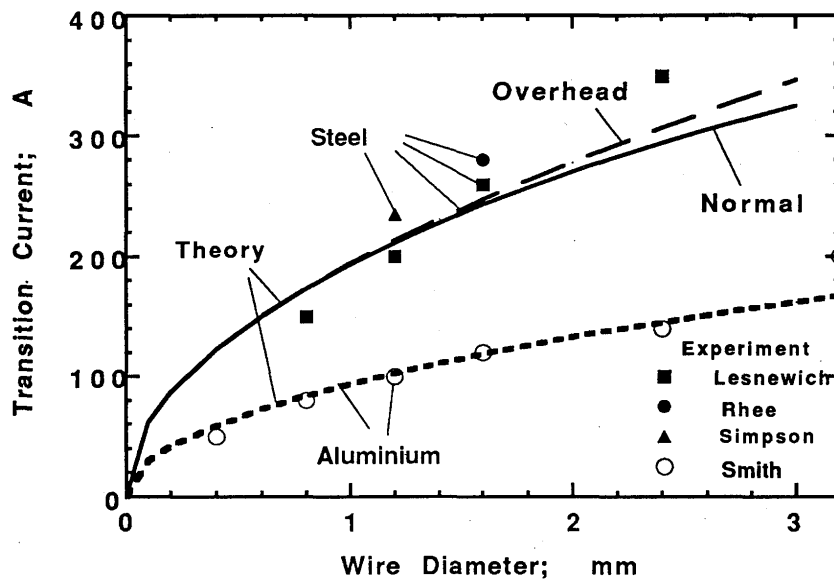


Fig.9 : Comparison of experimental results of transition current for spray transfer with predictions from the approximate formula [21].

### Acknowledgments.

The author is most indebted to his colleagues and coworkers of the CSIRO Division of Applied Physics, namely Tony Farmer, Gerry Haddad, Jawad Haidar, Dick Morrow and Tony Murphy, on whose work the present paper depends.

### References

- 1) M. Ushio and F. Matsuda: *Trans. JWRI*, 11 (1981), p.7.
- 2) A. Matsunawa, S.Yokoya and Y.Asako: *Trans. JWRI*, 16 (1987),P.I-8.
- 3) A.J. Russo, R.L. Akau and J.L. Jellison: *Welding Journal*, 69 (1990), p. 23-S.
- 4) R.W. Hamming: *Numerical Methods for Scientists and Engineers*, McGraw-Hill. (1973), p. 4.
- 5) P. Zhu, JJ. Lowke, R. Morrow, and J. Haidar *J. Phys. D:APPL. Phys.* 28 (1995), p. 1369.
- 6) J.J. Lowke, R. Morrow and J. Haidar: *Proc. 12th Inter. Conf. Plasma Chemistry*, Minneapolis, (1995),p,1449, to be submitted to *J. Phys.D.Appl. Phys.*
- 7) J.J. Lowke and J.C. Quartel: submitted to *Aust. J. Phys.*: *Proc. 11 th Int. Conf. on Gas Discharges and their Applications*, Tokyo, (1995), p. 90.
- 8) X. Zhou and J. Heberlein: *Plasma Sources Sc.* 3 (1994), p. 564.
- 9) M.S. Benilov and A. Marotta: *J. Phys. D:Appl. Phys.* 28 (1995), p. 1869.
- 10) S. G. Starling and A. J. Woodall: *Physics*, Longmans, (1958), P104.
- 11) J.J. Lowke, R. Morrow, J. Haidar, and A.B. Murphy: submitted to *IEEE Trans. Plasma Science*.
- 12) J. F. Lancaster, J.F.: *The Physics of Welding*, Pergamon Press (1984), p. 234.
- 13) J. Haidar and J.J. Lowke: *J.Phys.D:Appl. Phys. and J. High Temp. Chem. Process.* accepted for publication.
- 14) J. Haidar and AJ.D. Farmer: *J. Phys. D.Appl. Phys.* 28 (1995), p. 2089.
- 15) H. Maecker: *Z. Phys.* 141(1955),p. 198.
- 16) A. Lesnewitch: *Welding Journal*, 37 (1958), p.418-S.
- 17) S. Rhee and E. Kannatey-Asibu: *Welding Journal*, 70 (1992), p.381-S.
- 18) S. I. Simpson, P. Zhu and M. Rados: *Proc. 42nd National Welding Conference*, Welding Technology Inst. Australia, Melbourne, 2 (1994) p. 31.1.
- 19) A. A. Smith and J. G. Poley: *British Welding Journal*, 6 (1959). p. S65.
- 20) E. A. Brandes Ed.: *Smithells Metals Reference Book*, 6th Ed., Butterworths [1983].
- 21) J.J. Lowke: submitted to the *Welding Journal*.